Imposing a magnetic field across a nonaxisymmetric shear layer in a rotating spherical shell

Rainer Hollerbach[a)]
Department of Mathematics, University of Exeter, Exeter, EX4 4QE, United Kingdom

(Received 5 November 1993; accepted 9 March 1994)

In the context of the generation of the Earth's magnetic field, nonaxisymmetric solutions of the forced momentum equation in a rotating spherical shell are considered in the inertia-less, inviscid limit. It has previously been pointed out that, in general, such solutions are singular, with all three flow components discontinuous across the cylinder tangent to the inner core and parallel to the axis of rotation. An integral constraint on the forcing was derived, which must be satisfied if the inviscid solution is to be nonsingular, and it was suggested that in the presence of a magnetic field the Lorentz force would adjust to satisfy this constraint, thereby eliminating the need for the viscous shear layer, which otherwise resolves the singularity. In this work an axisymmetric field is imposed across this shear layer, and it is demonstrated that for a sufficiently strong field this adjustment does indeed occur.

I. INTRODUCTION

The Earth's magnetic field is created by fluid motions in its liquid iron outer core. Obtaining solutions of the coupled momentum and induction equations in a rotating spherical shell is thus of some interest. The suitably nondimensionalized equations for the magnetic field **B** and the fluid flow **U** are[1]

$$\text{Ro}\,\frac{D\mathbf{U}}{Dt}+2\hat{\mathbf{k}}\times\mathbf{U}=-\nabla p+\epsilon\,\nabla^2\mathbf{U}+\Theta\mathbf{r}+(\nabla\times\mathbf{B})\times\mathbf{B}, \tag{1}$$

$$\frac{\partial\mathbf{B}}{\partial t}=\nabla^2\mathbf{B}+\nabla\times(\mathbf{U}\times\mathbf{B}). \tag{2}$$

These, together with an equation for the buoyancy Θ, which will not be considered here though, govern the evolution of the geodynamo. The magnetic field and the buoyancy have been normalized in such a way that the Lorentz and buoyancy forces in (1) are comparable to the Coriolis force; the fluid flow has been normalized in such a way that the diffusive and inductive time scales in (2) are comparable.

Probably the single most important feature of the geodynamo is the dominance of rotation, and the corresponding smallness of the Rossby and Ekman numbers. The Rossby number $\text{Ro}=\eta/\Omega L^2$ is a measure of the rotational time scale Ω^{-1} to the Ohmic time scale L^2/η, and is $O(10^{-8})$. The Ekman number $\epsilon=\nu/\Omega L^2$ is a measure of viscous to Coriolis forces, and is $O(10^{-15})$. Here Ω is the Earth's rotation rate, L is a typical length scale such as the core radius, and η and ν are, respectively, the magnetic diffusivity and viscosity of the fluid. Coping with the smallness of these two nondimensional numbers is what makes a direct solution of the geodynamo equations so difficult that it has hitherto proved intractable. Setting $\text{Ro}=0$ and thereby focusing only on the slow evolution poses no great difficulty, although it does change the mathematical nature of the momentum equation. It is attempting to set $\epsilon=0$ as well that poses considerable difficulties, one of which I will address in this work.

It is well known that attempting to set $\epsilon=0$ in the axisymmetric component of (1) results in Taylor's constraint,[2] requiring the integrated Lorentz torque on concentric cylinders parallel to the axis of rotation to vanish on each such cylinder. How the mean field and flow adjust to this constraint in the limit $\epsilon\to 0$ has been the subject of no less than three Ph.D. theses.[3–5]

In contrast, in the so-called magnetoconvection problem, in which the axisymmetric components **B** and **U** are assumed given, and one considers the linearized nonaxisymmetric perturbations **b** and **u** (from now on, capital letters will denote axisymmetric quantities, and lowercase letters nonaxisymmetric quantities), it has generally been assumed that one can set $\epsilon=0$ without difficulty. While this turns out to be true in a sphere,[6] it is not so in a spherical shell.

It has recently been pointed out[7] that, in general, nonaxisymmetric solutions of the inertia-less inviscid momentum equation in a rotating spherical shell are singular, with all three components of the flow discontinuous across the cylinder tangent to the inner core and parallel to the axis of rotation. This singularity can be avoided if the forcing satisfies a particular constraint, and it was suggested that the Lorentz force would, in fact, adjust to satisfy this constraint, thereby eliminating the need for the viscous shear layer that must otherwise resolve the singularity. In this work it is demonstrated that this adjustment does occur, at least in the presence of an imposed axisymmetric field whose component perpendicular to the shear layer is nowhere zero.

Briefly reviewing the essence of Ref. 7, consider the inertia-less inviscid momentum equation

$$2\hat{\mathbf{k}}\times\mathbf{u}=-\nabla p+\mathbf{f}, \tag{3}$$

where for now **f** is simply some given forcing, having the azimuthal dependence $\exp(im\phi)$, which factor will henceforth be implicit throughout. Taking the curl of (3), and using $\nabla\cdot\mathbf{u}=0$, one obtains

$$-2\,\frac{\partial}{\partial z}\,\mathbf{u}=\nabla\times\mathbf{f}, \tag{4}$$

which then implies

[a)]Present address: Institute of Geophysics and Planetary Physics, Los Alamos National Laboratory, Los Alamos, New Mexico 87545.

 1070-6631/94/6(7)/2540/5/$6.00

$$\mathbf{u}=-\frac{1}{2}\int^{z}\nabla\times\mathbf{f}\,dz'+\mathbf{c}(s), \tag{5}$$

where (z,s,ϕ) are cylindrical coordinates. Letting subscripts denote the indicated components, two boundary conditions on appropriate linear combinations of u_z and u_s will turn out to determine c_z and c_s. For the nonaxisymmetric modes $m\neq 0$, c_ϕ is then determined by requiring that $\nabla\cdot\mathbf{u}=0$ once again.

The reason this seemingly straightforward algorithm for determining the constants of integration $\mathbf{c}(s)$ breaks down when applied in a spherical shell lies in the boundary conditions that must be applied to determine c_z and c_s: At the outer boundary the no-normal-flow boundary condition becomes

$$zu_z+su_s=0,\quad \text{at } z=(r_o^2-s^2)^{1/2}, \tag{6}$$

and this applies for all $s\leqslant r_o$. At the inner boundary, the no-normal-flow boundary condition becomes

$$zu_z+su_s=0,\quad \text{at } z=(r_i^2-s^2)^{1/2}, \tag{7a}$$

but this applies only for $s\leqslant r_i$. For $r_i\leqslant s\leqslant r_o$, we take, instead, the symmetry condition

$$u_z=0,\quad \text{at } z=0, \tag{7b}$$

appropriate for solutions having u_z antisymmetric and u_s and u_ϕ symmetric about the equator. The point now is that (7a) and (7b) do not join smoothly at $s=r_i$, $z=0$, where (7a) becomes $u_s=0$ instead of $u_z=0$. This discontinuity in the applied boundary conditions will then induce a discontinuity in the constants of integration c_z and c_s, and according to (5) this discontinuity will manifest itself in the flow for all z on the tangent cylinder at $s=r_i$.

If one really believes the $\epsilon\equiv 0$ limit to be appropriate, the only resolution to this singularity is to assume that $\mathbf{f}$ satisfies some condition that ensures that c_z and c_s just happen to be continuous. After all, for *some* $\mathbf{f}$ it must surely be the case that both u_z and u_s are zero at $s=r_i$, $z=0$, and if that is the case then (7a) and (7b) will join somewhat more smoothly. But if u_z and u_s are both to be zero at $s=r_i$, $z=0$, c_z and c_s are completely specified at $s=r_i$. And yet this flow must still satisfy the outer boundary condition (6), which then turns out to give us the constraint on $\mathbf{f}$,

$$z\int_0^z(\nabla\times\mathbf{f})_z dz'+s\int_0^z(\nabla\times\mathbf{f})_s\,dz'=0, \tag{8}$$

which must be satisfied at $s=r_i$, $z=(r_o^2-r_i^2)^{1/2}$. If (8) is not satisfied, the solution (5), although well defined and unique, will have a very severe singularity across the tangent cylinder at $s=r_i$, which must be resolved by a viscous shear layer, that is, by carefully considering the limit $\epsilon\rightarrow 0$ instead of $\epsilon\equiv 0$.

II. MAGNETIC COUPLING

In Ref. 7, we simply took $\mathbf{f}$ to be some given, fixed forcing, which either did or did not satisfy (8), and examined the structure of the numerically computed shear layer. (Incidentally, the details of the numerical solution, which were not presented there, are provided in the Appendix here.) However, in the proper geophysical context, $\mathbf{f}$ should not be taken to be some fixed forcing. Instead, as in (1), it is itself a dynamic variable, consisting of the buoyancy force ultimately responsible for driving the fluid motion, as well as the Lorentz force exerted by the magnetic field. And considering the stiffening effect that this Lorentz force has on the fluid, it seems rather unlikely that the magnetic field would tolerate strong shear layers in the interior of a conducting fluid. So, we postulated that, starting from some initial configuration in which the forcing does not satisfy (8), the flow would distort the field into a configuration in which it does.

To test this idea, I consider the following idealized model: In Ref. 7, we solved the momentum equation,

$$2\hat{\mathbf{k}}\times\mathbf{u}=-\nabla p+\epsilon\,\nabla^2\mathbf{u}+\mathbf{f}, \tag{9}$$

in the limit of small ϵ, where again $\mathbf{f}$ was just some given, fixed forcing. To provide a dynamic coupling between $\mathbf{f}$ and $\mathbf{u}$, I begin by imposing a given axisymmetric magnetic field $\mathbf{B}$. The nonaxisymmetric flow $\mathbf{u}$ driven by (9) will then act on $\mathbf{B}$ to induce a nonaxisymmetric field $\mathbf{b}$ via the induction equation (2),

$$\frac{\partial\mathbf{b}}{\partial t}=\nabla^2\mathbf{b}+\nabla\times(\mathbf{u}\times\mathbf{B}). \tag{10}$$

Note that because I am not imposing an axisymmetric fluid flow $\mathbf{U}$, there is no corresponding $\nabla\times(\mathbf{U}\times\mathbf{b})$ term. The linearized Lorentz force generated by the interaction of $\mathbf{B}$ and $\mathbf{b}$ will then modify the force $\mathbf{f}$ to

$$\mathbf{f}=\mathbf{f}_0+\Lambda[(\nabla\times\mathbf{B})\times\mathbf{b}+(\nabla\times\mathbf{b})\times\mathbf{B}], \tag{11}$$

where only $\mathbf{f}_0$ is now the given, fixed force, and the Elsässer number Λ is a measure of the strength of the imposed field $\mathbf{B}$. Thus, by increasing Λ from zero, I allow for dynamic coupling between $\mathbf{f}$ and $\mathbf{u}$, and the hypothesis is then that as Λ is increased and ϵ is decreased, the *total* force $\mathbf{f}$ will adjust to satisfy (8).

III. RESULTS

I take for the imposed force $\mathbf{f}_0=(-4isz\hat{\mathbf{e}}_z+2is^2\hat{\mathbf{e}}_s)\exp(i\phi)$, as in example 1 of Ref. 7. One may easily verify that the inviscid solution (5) is

$$u_z=-sz+c_z(s),\quad u_s=-z^2+c_s(s),$$
$$u_\phi=-i(z^2+s^2)+c_\phi(s). \tag{12}$$

From (6) and (7), the constants of integration then turn out to be, for $s<r_i$,

$$c_z=2s[(r_o^2-s^2)^{1/2}+(r_i^2-s^2)^{1/2}],$$
$$c_s=-2(r_o^2-s^2)^{1/2}(r_i^2-s^2)^{1/2}, \tag{13a}$$
$$c_\phi=-2i[r_o^2r_i^2-2s^2(r_o^2+r_i^2)+3s^4]/(r_o^2-s^2)^{1/2}(r_i^2-s^2)^{1/2},$$

and for $s>r_i$,

$$c_z=0,\quad c_s=2(r_o^2-s^2),$$
$$c_\phi=2i(r_o^2-3s^2). \tag{13b}$$

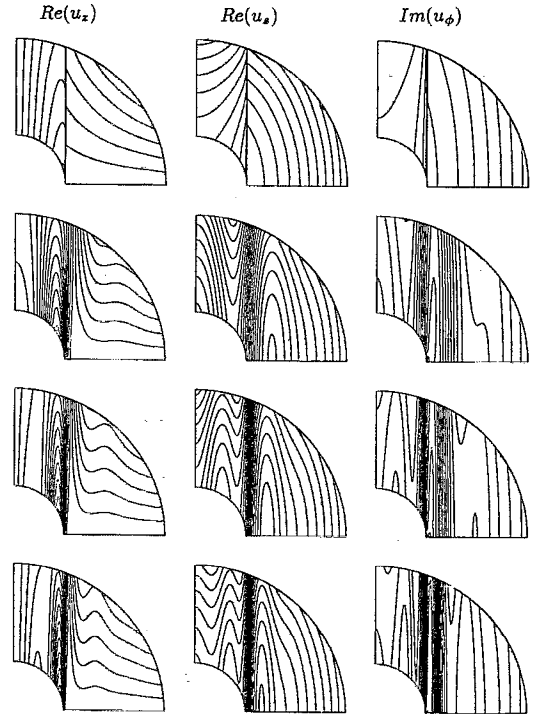

FIG. 1. At the top, the inviscid solution (12) corresponding to $\mathbf{f}_0$. Below, the viscous solutions at $\epsilon=10^{-4}$, $10^{-4.5}$, and 10^{-5}. From left to right, the real parts of u_z and u_s, and the imaginary part of u_ϕ. Contour intervals of 0.2 for u_z, 0.4 for u_s, and 2 for u_ϕ.

One notes that c_z and even c_s are discontinuous across $s=r_i$, and $c_\phi \to \infty$ as $s \to r_i^-$. And indeed, if one evaluates the constraint (8), one obtains not 0, but

$$\left| z\int_0^z (\nabla\times\mathbf{f}_0)_z \, dz' + s\int_0^z (\nabla\times\mathbf{f}_0)_s \, dz' \right| = 4, \tag{14}$$

taking the radii of the spherical shell to be $r_i=\frac{1}{2}$, $r_o=\frac{3}{2}$. This (formally valid) inviscid solution thus has little meaning in the vicinity of $s=r_i$. Figure 1 shows the singularity in the inviscid solution, as well as how the viscous solution at Ekman numbers of 10^{-4}, $10^{-4.5}$, and 10^{-5} resolves the singularity. Shown in Fig. 1 are the real parts of u_z and u_s, and the imaginary part of u_ϕ. For this particular example, the inviscid solution has u_z and u_s purely real, and u_ϕ purely imaginary. The inclusion of viscosity destroys this phase relationship, but the out-of-phase component displays a similar boundary layer structure, and of course vanishes sufficiently far from $s=r_i$.

The boundary layer in the viscous solutions is quite strong, and evidently rather slowly convergent, considering how far from $s=r_i$ one must go before the solution resembles the inviscid solution, even at $\epsilon=10^{-5}$. The detailed structure appears to consist of several nested layers, not unlike the classical axisymmetric Stewartson[8] layer, which consists of three nested layers of innermost thickness $\epsilon^{1/3}$ and outer thicknesses $\epsilon^{2/7}$ and $\epsilon^{1/4}$. The purpose of the Stewartson layer, however, is quite different, and so one should not expect the structure to be identical. In particular, one main function of the Stewartson layer is to provide a mass flux balance between the inner and outer Ekman layers. In contrast, one notes that the shear layer obtained here is essentially independent of any Ekman layers; indeed, I specifically imposed stress-free boundary conditions at r_i and r_o to minimize the effects of any Ekman layers. Also, unlike the shear layer here, whose main function is precisely to accommodate the discontinuity in the normal component of the flow, the Stewartson layer involves no discontinuity in the normal component. For example, note in Fig. 1 how the azimuthal component u_ϕ becomes increasingly large just inside the tangent cylinder as ϵ becomes small, in agreement with the inviscid result $c_\phi \to \infty$ as $s \to r_i^-$. Such features are entirely absent in the axisymmetric Stewartson layer, precisely because it involves no discontinuity in the normal component of the flow.

TABLE I. The quantity $\frac{1}{4}|z\int_0^z(\nabla\times\mathbf{f})_z\,dz'+s\int_0^z(\nabla\times\mathbf{f})_s\,dz'|$, evaluated for $s=r_i$, $z=(r_o^2-r_i^2)^{1/2}$, as a function of Λ and ϵ.

Λ	0	1/2	1	3/2	2
$\epsilon=10^{-4}$	1.00	0.54	0.17	0.08	0.04
$\epsilon=10^{-4.5}$	1.00	0.49	0.12	0.05	0.02
$\epsilon=10^{-5}$	1.00	0.42	0.08	0.02	<0.01

As noted above, here I am not content in merely pointing out the existence of this singularity and the viscous shear layer that resolves it in the nonmagnetic regime; I am also interested in the effect that a perpendicularly applied magnetic field might have on this shear layer. (It is intuitively plausible that the normal component of the field will have the greatest effect. For example, it is known that an order one magnetic field will suppress the axisymmetric Stewartson layer if it is normal,[9] but not if it is tangential.[10]) So, I take, for the imposed axisymmetric field $\mathbf{B}=2s\hat{\mathbf{e}}_s-4z\hat{\mathbf{e}}_z$, having the so-called quadrupolar symmetry about the equator. The Earth's magnetic field is, in fact, predominantly dipolar, so in a sense this is the geophysically "wrong" parity. However, this particular field has the very considerable advantage that its component perpendicular to the shear layer is constant over the whole shear layer, that is, $B_s=1$ everywhere on the inner core tangent cylinder $s=r_i$. Any dipolar field would necessarily have $B_s=0$ at the equator. Incidentally, for this particular symmetry of $\mathbf{B}$, it then turns out that $\mathbf{b}$ must have the same symmetry as $\mathbf{u}$.

Table I shows the quantity

$$\frac{1}{4}\left| z\int_0^z (\nabla\times\mathbf{f})_z \, dz' + s\int_0^z (\nabla\times\mathbf{f})_s \, dz' \right|, \tag{15}$$

as it depends on Λ and ϵ. According to (14), for $\Lambda=0$ this quantity is exactly one for all ϵ, since there is no magnetic adjustment. However, for $\Lambda=O(1)$, this quantity does increasingly adjust to zero as ϵ becomes small. Indeed, for $\Lambda=2$ and $\epsilon=10^{-5}$, it is less than 0.01, so small that it can no longer be reliably evaluated at the truncation used here. Thus, it is quite clear that for sufficiently strong magnetic coupling between $\mathbf{f}$ and $\mathbf{u}$, $\mathbf{f}$ does indeed adjust to satisfy (8) as ϵ is decreased. Correspondingly, there should no longer be a shear layer in the solutions. Figures 2 and 3 show the flow $\mathbf{u}$ and the current density $\mathbf{j}=\nabla\times\mathbf{b}$ for $\Lambda=2$, $\epsilon=10^{-4.5}$, and

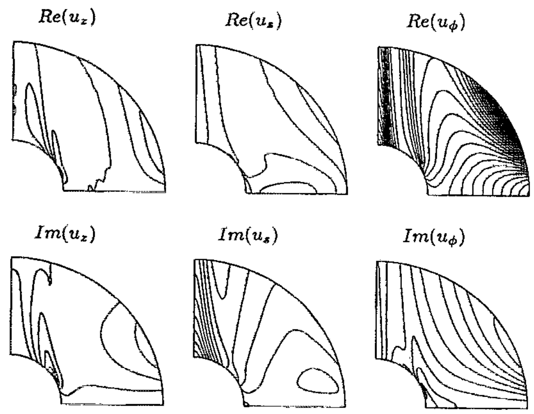

FIG. 2. The flow **u** for $\Lambda=2$, $\epsilon=10^{-4.5}$. Contour intervals of 0.04.

indeed there are no shear layers observable. Furthermore, unlike the nonmagnetic solutions in Fig. 1, this solution is essentially independent of ϵ; that is, the solution for ϵ equals 10^{-4} or 10^{-5} would look almost indistinguishable.

IV. CONCLUSION

In this work I have pointed out once again that, in general, nonaxisymmetric solutions of the forced momentum equation in a rotating spherical shell are singular in the inertia-less, inviscid limit, with all three flow components discontinuous across the inner core tangent cylinder. In the nonmagnetic regime, where there is no dynamic coupling between **f** and **u**, this singularity can only be accommodated by a viscous shear layer, and viscosity is thus essential in obtaining sensible nonaxisymmetric solutions. In contrast, in the magnetic regime, where there is dynamic coupling between **f** and **u**, this singularity is accommodated by an adjustment in **f** to satisfy a particular integral constraint, and viscosity is thus not essential.

Nevertheless, one should be extremely cautious about neglecting viscosity entirely. An immediate consequence of setting ϵ to zero *identically* is that **f** *must* also satisfy (8) *identically*. While the presence of the magnetic field effectively removes the singularity associated with the tangent cylinder, the price one pays is the need to satisfy the constraint (8). However, one cannot solve for **u** and **f** as before in a sphere,[6] and merely impose (8) as an additional constraint, for the system would then be overdetermined. The need to satisfy (8) requires an adjustment throughout the whole interior (note how the solution in Fig. 2 is quite distinct from either the inviscid or the viscous solutions in Fig. 1). One would have to solve for **u** and **f** self-consistently in such a way that (8) just happens to be satisfied, and it is not quite clear (to me at any rate) how one might do that. It is probably easiest computationally to include viscosity, as has been done here, and allow this dynamic adjustment to sort itself out.

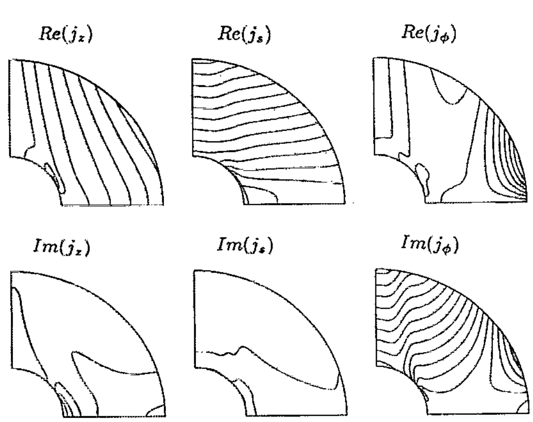

FIG. 3. The current density **j** for $\Lambda=2$, $\epsilon=10^{-4.5}$. Contour intervals of 0.04.

ACKNOWLEDGMENTS

I thank Dr. M. R. E. Proctor, Dr. C. A. Jones, and Dr. G. A. Glatzmaier for valuable discussions. This work was funded by the British SERC under Grant No. GR/E93251.

APPENDIX: NUMERICAL SOLUTION

We begin by decomposing **b** as

$$\mathbf{b}=\nabla\times(g\hat{\mathbf{r}})+\nabla\times\nabla\times(h\hat{\mathbf{r}}), \tag{A1}$$

thereby satisfying $\nabla\cdot\mathbf{b}=0$. We then expand g and h as [remember there is also an implicit factor of $\exp(im\phi)$]

$$g(r,\theta)=\sum_{j=1}^{N_1} g_j(r)P_{n_1}^m(\cos\,\theta)$$

$$=\sum_{j=1}^{N_1}\sum_{k=1}^{M_1+2} g_{jk}T_{k-1}(x)P_{n_1}^m(\cos\,\theta), \tag{A2a}$$

$$h(r,\theta)=\sum_{j=1}^{N_1} h_j(r)P_{n_2}^m(\cos\,\theta)$$

$$=\sum_{j=1}^{N_1}\sum_{k=1}^{M_1+2} h_{jk}T_{k-1}(x)P_{n_2}^m(\cos\,\theta), \tag{A2b}$$

where (r,θ,ϕ) are spherical coordinates. Here $P_n^m(\cos\,\theta)$ are associated Legendre polynomials, with $n_1=2j+m-1$, $n_2=2j+m-2$ (it is here that we impose the appropriate symmetry about the equator). Here $T_{k-1}(x)$ are Chebyshev polynomials, and

$$r=\frac{r_o+r_i}{2}+\frac{r_o-r_i}{2}x \tag{A3}$$

determines x, the radial coordinate normalized to $(-1,1)$ across the gap.

The r components of (10) and its curl then yield

$$\sum_{j=1}^{N_1} n_2(n_2+1)\left(\frac{\partial}{\partial t}-L_{n_2}\right)\left(\frac{h_j}{r^2}\right)P_{n_2}^m(\cos\,\theta)=\hat{\mathbf{r}}\cdot\nabla\times(\mathbf{u}\times\mathbf{B}), \tag{A4a}$$

$$\sum_{j=1}^{N_1} n_1(n_1+1)\left(\frac{\partial}{\partial t}-L_{n_1}\right)\left(\frac{g_j}{r^2}\right)P_{n_1}^m(\cos\,\theta)$$

$$=\hat{\mathbf{r}}\cdot\nabla\times\nabla\times(\mathbf{u}\times\mathbf{B}), \tag{A4b}$$

where the operator

$$L_n=\frac{1}{r^2}\frac{d^2}{dr^2}r^2-\frac{n(n+1)}{r^2}. \tag{A5}$$

Equations (A4) are then time stepped to equilibrium by a second-order Runge–Kutta method, modified to treat the diffusive terms implicitly. The inductive calculations on the right-hand side are done pseudospectrally in the angular coordinate, and by collocation in the radial coordinate, at the M_1 zeros of $T_{M_1}(x)$ on $(-1,1)$. The "extra" coefficients, $k=M_1+1,\ M_1+2$ in (A2), are determined by the two boundary conditions at r_i and r_o. The boundary conditions we impose on g_j and h_j are

$$g_j=0,\quad \text{at } r=r_i,\ r_o, \tag{A6a}$$

$$\left(\frac{d}{dr}-\frac{n_2+1}{r}\right)h_j=0,\quad \text{at } r=r_i, \tag{A6b}$$

$$\left(\frac{d}{dr}+\frac{n_2}{r}\right)h_j=0,\quad \text{at } r=r_o, \tag{A6c}$$

for each j. These are the appropriate boundary conditions for an insulator in the regions $r\leqslant r_i$ and $r\geqslant r_o$.

We similarly decompose $\mathbf{u}$ as

$$\mathbf{u}=\nabla\times(e\hat{\mathbf{r}})+\nabla\times\nabla\times(f\hat{\mathbf{r}}), \tag{A7}$$

and expand e and f as

$$e(r,\theta)=\sum_{j=1}^{N_2} e_j(r)P_{n_1}^m(\cos\theta)=\sum_{j=1}^{N_2}\sum_{k=1}^{M_2+2} e_{jk}T_{k-1}(x)P_{n_1}^m(\cos\theta), \tag{A8a}$$

$$f(r,\theta)=\sum_{j=1}^{N_2} f_j(r)P_{n_2}^m(\cos\theta)=\sum_{j=1}^{N_2}\sum_{k=1}^{M_2+4} f_{jk}T_{k-1}(x)P_{n_2}^m(\cos\theta). \tag{A8b}$$

Incidentally, the truncation used in this work is $N_1=25$, $M_1=30$, and $N_2=50$, $M_2=60$.

The r components of the curl and the curl of the curl of (9) then yield

$$-\sum_{j=1}^{N_2}[2im+\epsilon n_1(n_1+1)L_{n_1}]\left(\frac{e_j}{r^2}\right)P_{n_1}^m(\cos\theta)+\sum_{j=1}^{N_2}\frac{2}{r^2}\left(\frac{n_2(n_2+1)}{r}-\frac{d}{dr}\right)f_j\sin\theta\frac{d}{d\theta}P_{n_2}^m(\cos\theta)+\sum_{j=1}^{N_2}\frac{2}{r^2}n_2(n_2+1)\left(\frac{2}{r}-\frac{d}{dr}\right)f_j\cos\theta P_{n_2}^m(\cos\theta)=\hat{\mathbf{r}}\cdot\nabla\times\mathbf{f}, \tag{A9a}$$

$$\sum_{j=1}^{N_2}[2im+\epsilon n_2(n_2+1)L_{n_2}]L_{n_2}\left(\frac{f_j}{r^2}\right)P_{n_2}^m(\cos\theta)+\sum_{j=1}^{N_2}\frac{2}{r^2}\left(\frac{n_1(n_1+1)}{r}-\frac{d}{dr}\right)e_j\sin\theta\frac{d}{d\theta}P_{n_1}^m(\cos\theta)+\sum_{j=1}^{N_2}\frac{2}{r^2}n_1(n_1+1)\left(\frac{2}{r}-\frac{d}{dr}\right)e_j\cos\theta P_{n_1}^m(\cos\theta)=\hat{\mathbf{r}}\cdot\nabla\times\nabla\times\mathbf{f}. \tag{A9b}$$

Using the appropriate recursion relations,[11] one can show that both $\sin\theta(d/d\theta)P_n^m(\cos\theta)$ and $\cos\theta P_n^m(\cos\theta)$ are, in fact, linear combinations only of $P_{n\pm1}^m(\cos\theta)$. Thus, (A9a) couples e_j only to f_j and f_{j+1}, and (A9b) couples f_j only to e_{j-1} and e_j. The structure of the system one must solve at each time step of (A4) to obtain the e_{jk}'s and f_{jk}'s is thus block tridiagonal, and one proceeds exactly as outlined[9] for the axisymmetric case. The details of what goes into the various blocks is, of course, somewhat more involved, particularly as both the e_{jk}'s and f_{jk}'s, as well as the matrix to be inverted, are now complex, but the basic solution strategy is the same.

Finally, in order to minimize the effects of any Ekman boundary layers, we use stress-free boundary conditions,

$$u_r=\frac{\partial}{\partial r}\left(\frac{u_\theta}{r}\right)=\frac{\partial}{\partial r}\left(\frac{u_\phi}{r}\right)=0,\quad \text{at } r=r_i,\ r_o, \tag{A10a}$$

which become in terms of the e_j's and f_j's

$$f_j=\frac{d}{dr}\left(\frac{1}{r^2}\frac{d}{dr}f_j\right)=\frac{d}{dr}\left(\frac{1}{r^2}e_j\right)=0,\quad \text{at } r=r_i,\ r_o, \tag{A10b}$$

for each j, and are again incorporated into the appropriate blocks as before.[9]

[1] D. R. Fearn, "Nonlinear planetary dynamos," in *Lectures on Solar and Planetary Dynamos*, edited by M. R. E. Proctor and A. D. Gilbert (Cambridge University Press, Cambridge, 1993).
[2] J. B. Taylor, "The magnetohydrodynamics of a rotating fluid and the Earth's dynamo problem," Proc. R. Soc. London Ser. A **274**, 274 (1963).
[3] M. R. E. Proctor, "Nonlinear mean field dynamo models and related topics," Ph.D. thesis, University of Cambridge, 1975.
[4] G. R. Ierley, "Macrodynamics of α-dynamos," Ph.D. thesis, Massachusetts Institute of Technology, 1982.
[5] R. Hollerbach, "α-effect dynamos and Taylor's constraint in the asymptotic limit of small viscosity," Ph.D. thesis, Scripps Institution of Oceanography, 1990.
[6] D. R. Fearn and W. S. Weiglhofer, "Magnetic instabilities in rapidly rotating spherical geometries," Geophys. Astrophys. Fluid Dyn. **67**, 163 (1992).
[7] R. Hollerbach and M. R. E. Proctor, "Non-axisymmetric shear layers in a rotating spherical shell," in *Theory of Solar and Planetary Dynamos*, edited by M. R. E. Proctor, P. C. Matthews, and A. M. Rucklidge (Cambridge University Press, Cambridge, 1993).
[8] K. Stewartson, "On almost rigid rotations," J. Fluid Mech. **26**, 131 (1966).
[9] R. Hollerbach, "Magnetohydrodynamic Ekman and Stewartson layers in a rotating spherical shell," Proc. R. Soc. London Ser. A **444**, 333 (1994).
[10] D. B. Ingham, "Magnetohydrodynamic flow in a container," Phys. Fluids **12**, 389 (1969).
[11] M. Abramowitz and I. A. Stegun, (Editors), *Handbook of Mathematical Functions* (Dover, New York, 1968).